Nonlinear electrostriction in the mixed ferroelectric $KTa_{1-x}Nb_xO_3$

J. Toulouse and R. K. Pattnaik
Physics Department, Lehigh University, Bethlehem, Pennsylvania 18015
(Received 16 January 2001; revised manuscript received 23 August 2001; published 19 December 2001)

The dielectric resonance previously reported in the paraelectric phase of the mixed ferroelectric $KTa_{1-x}Nb_xO_3$ is studied quantitatively. A theoretical model is developed that incorporates a field-induced electrostrictive coupling mediated by polar nanoregions appearing above the transition, and their orientational relaxation. Theoretical expressions for the dielectric dispersion and absorption are calculated, fitted to the experimental data, and values are obtained for the electrostriction coefficient and the relaxation time of the polar regions. Starting approximately 5 K above the transition, and upon repetitive excitation, a remarkable growth in the resonance is observed, ending in a singular behavior where the resonance splits into two very sharp spikes. This observation is described in the framework of the model as a nonlinear electrostrictive effect.

DOI: 10.1103/PhysRevB.65.024107 PACS number(s): 77.80.−e, 77.22.Ej

I. INTRODUCTION

Mixed ferroelectrics have been the focus of much fundamental and applied research for several years. These are highly polarizable systems in which one of the lattice sites in the unit cell is occupied by either one of two different atomic species, which, in addition, can be displaced (off center) from the normal site. If displaced, the unit cell produces a dipolar field around it and, because of the strong polarizability of the lattice, surrounding host cells can also be polarized. The combined effects of several off-center ions eventually leads to the formation of polar nanoregions that can considerably modify the physical properties of mixed ferroelectric crystals, making them attractive for a variety of applications, and in particular, their electrostrictive properties for the design of efficient transducers and actuators. Höchli[1] and Vugmeister[2] have reviewed experimental and theoretical results on the subject.

Two systems are particularly useful as models for understanding the structural origin and fundamental mechanism of the collective effects in mixed ferroelectrics: they are $K_{1-x}Li_xTaO_3$ (KLT) and $KTa_{1-x}Nb_xO_3$ (KTN). These two systems are derived from the same incipient ferroelectric $KTaO_3$, which remains cubic at all temperatures. The origin of the peculiar collective behavior of these two systems lies in the fact that the Nb atom substituted for Ta, or Li substituted for K, is shifted away from the center of the unit cell[3] and exhibits a relaxational motion between equivalent sites, with a characteristic time that is temperature dependent.[1,2] The off-center occupancy has the effect of polarizing and distorting the surrounding host cells and leads to the formation of polar nanoregions giving rise to new and unexpected collective effects. For instance, first-order Raman scattering, forbidden by symmetry in the paraelectric phase, is already active above the phase transition in both KTN and KLT, clearly signaling the appearance of local precursor distortions in the crystal.[4–6] Also preceding the transition, the dielectric response is found[7] to exhibit the characteristic relaxor behavior and to depart from a Curie-Weiss law. A frequency-dependent remnant polarization is also revealed in the hysteresis loop measurements.[8] Finally, both KLT and KTN exhibit field-induced dielectric resonances above the transition.[9] These, in KTN, are the subject of the present paper.

As is well known,[10–12] a coupling between polarization and strain can give rise to dielectric resonances in crystals, the frequency of which is determined by the mechanical modes of vibrations of a particular sample. In a recent study, we showed that the dielectric resonance observed in KLT[9] is due to an electrostrictive coupling between polarization and strain mediated by the polar nanoregions that appear well above the transition. In that study, we calculated the dielectric dispersion and absorption, incorporating this polarization-strain coupling. Based on experimental measurements and theoretical calculations, we showed that, as the Li^+ relaxation frequency approaches the resonance frequency of the sample, the resonance becomes heavily damped and evolves into a relaxation.

The two systems, KLT and KTN, differ in an essential way: in KLT, the Li^+ relaxation falls in the kHz to MHz range, i.e., in the frequency range of the observed resonance, while, in KTN, all indications are that the Nb^{5+} relaxation lies in the GHz range, or well above the resonance frequencies in usual dielectric experiments. Application of the previous model[9] to the present KTN results confirms these indications. In the present paper, we also report quite an unexpected phenomenon observed in KTN. Close to but above the transition temperature, the loss tangent measured in repetitive frequency sweeps increases progressively and eventually, with time, splits into two extremely sharp spikes corresponding to a resonance and its antiresonance.

The paper is organized as follows. We first review the theoretical model[9] used to calculate the complex dielectric constant, which includes an electrostrictive polarization-strain coupling. This is followed by a report of the experimental dielectric-resonance results in KTN, application of the theoretical model to these results and, finally, discussion of the results.

II. ELECTROSTRICTIVE POLARIZATION-STRAIN COUPLING

In the high-temperature paraelectric phase, both KLT and KTN are macroscopically centrosymmetric. It is well known

that, under such conditions, a crystal cannot possess a macroscopic polarization and, hence, cannot exhibit a piezoelectric response. However, in KLT and KTN, the center of symmetry can easily be broken by the application of a dc bias field. The preferential alignment of the off-center ions and polar regions then induces a macroscopic polarization P_0 that can electrostrictively couple to the mechanical strain. If a small alternating electric field is superposed onto the dc bias field, the induced macroscopic polarization will oscillate about its dc value at the frequency of the small measuring ac field. The electrostrictive coupling then manifests itself as a resonance in the dielectric response of the sample when the appropriate conditions, discussed below, are met.

Let us consider a sample of length l, width w, and thickness d such that the length is much greater than the other two dimensions. Let the length be along the x axis, and the thickness along the z axis. The long surfaces ($l\times w$) are fully electroded and all the fields are applied across the thickness d. Since the width and thickness are much smaller than the length, it is a good approximation[10] to neglect the stresses across the thickness and width of the sample. With these assumptions, Mason and others have shown that, to first-order in the small ac field $\mathcal{E}(t)$, the time-dependent strain can be written as

$$S_1(x,t)=s_{11}^E T_1(x,t)+2M_{13}E_0\mathcal{E}(t). \tag{1}$$

Here S_1 is the strain, T_1 is the stress, s_{11}^E the elastic compliance at constant electric field, $M_{13}(=M_{1133})$ is the relevant electrostriction coefficient, E_0 the dc bias electric field inducing a polarization, $P_0=\chi_s E_0$ in which χ_s is the static susceptibility of the crystal, and $\mathcal{E}(t)$ the small ac measuring field. The first term on the right of Eq. (1) corresponds to Hooke's law and the second to the electrostrictive effect. The second term in Eq. (1) gives rise to a resonance in the dielectric response of the sample when the frequency of the exciting field $E_0(t)$ equals the frequency of the fundamental longitudinal acoustic mode propagating along the length of the sample. In the recent KLT study referenced above,[9] we extended the model of Mason[10] and others[11,12] to include the contribution of an impurity relaxation (in the Debye approximation) and a strain-rate-dependent damping. An overview of the model is given below, highlighting its main points:

The elastic wave equation for the particle displacement, $u(x,t)$, in one dimension is[13]

$$\rho\frac{\partial^2 u(x,t)}{\partial t^2}=\frac{1}{s_{11}^E}\frac{\partial^2 u(x,t)}{\partial x^2}+\eta\frac{\partial}{\partial t}\frac{\partial^2 u(x,t)}{\partial x^2}, \tag{2}$$

where ρ is the density and η is an effective viscosity responsible for the damping. Solving Eq. (2) with stress-free boundary conditions, $T(\pm l/2)=0$, leads to the following expression for the stress:[10,9]

$$T(x,t)=\frac{2E_0M_{13}}{s_{11}^E}\left\{\frac{\cos k_c x}{\cos k_c l/2}-1\right\}\mathcal{E}(t), \tag{3}$$

where k_c is the complex wave vector of the longitudinal sound wave propagating with speed V and frequency ω along the length of the bar sample. The expression $k_c l/2$ is given by[13]

$$\frac{k_c l}{2}=\frac{\omega l}{2V}-i\frac{\eta\omega^2 l s_{11}^E}{4V}=\theta-i\beta, \tag{4}$$

where θ and β are the abbreviations

$$\theta(\omega)\equiv\frac{\omega l}{2V},\quad \beta(\omega)\equiv\frac{\eta\omega^2 l}{4V^3\rho}, \tag{5}$$

and we have used the relation $V^2=(\rho s_{11}^E)^{-1}$.

Next, we write the equation for the time evolution of the electric displacement $\mathcal{D}$ including a polarization-strain or electrostrictive coupling term and taking into account the impurity relaxation[9]

$$\frac{d\mathcal{D}}{dt}+\frac{1}{\tau}\mathcal{D}=\frac{1}{\tau}[\epsilon\mathcal{E}(t)+2M_{13}E_0T_1(x,t)], \tag{6}$$

where τ is the relaxation time associated with the impurity reorientation and ϵ is the permittivity of the medium.

The complex permittivity can then be deduced from Eq. (6) and without going into the details of this deduction, which are given elsewhere,[9] we directly quote the results for the real part (ϵ') and imaginary part (ϵ'') of the complex permittivity

$$\epsilon'(\omega)=\frac{\epsilon_s+\epsilon_\infty\omega^2\tau^2}{\omega^2\tau^2+1}-\left(\frac{4E_0^2M_{13}^2}{s_{11}^E}\right)\frac{1-Y_r(\omega)-\omega\tau Y_i(\omega)}{\omega^2\tau^2+1}, \tag{7}$$

$$\epsilon''(\omega)=\frac{(\epsilon_s-\epsilon_\infty)\omega\tau}{\omega^2\tau^2+1}-\left(\frac{4E_0^2M_{13}^2}{s_{11}^E}\right)\frac{\omega\tau-\omega\tau Y_r(\omega)+Y_i(\omega)}{\omega^2\tau^2+1}. \tag{8}$$

Here ϵ_s and ϵ_∞ are, respectively, the static and optical permittivities. The functions Y_r and Y_i represent the real and imaginary parts of the electrostrictive strain contribution, averaged over the length of the sample. This calculation has been carried out in the above cited reference[9] leading to the following expressions for Y_r and Y_i:

$$Y_r(\omega)=\frac{\theta\sin\theta\cos\theta+\beta\sinh\beta\cosh\beta}{(\theta^2+\beta^2)(\cos^2\theta+\sinh^2\beta)}, \tag{9}$$

$$Y_i(\omega)=\frac{\theta\sinh\beta\cosh\beta-\beta\sin\theta\cos\theta}{(\theta^2+\beta^2)(\cos^2\theta+\sinh^2\beta)}, \tag{10}$$

where θ and β defined in Eq. (5) are functions of ω.

In the work of Mason[10] and others,[11,12] the relaxation was assumed instantaneous and, therefore, the $d\mathcal{D}/dt$ term in Eq. (6) was absent. Also note that, for $E_0=0$, the polarization-strain coupling terms in Eq. (7) and Eq. (8) vanish, leading to the usual expressions for the Debye dielectric dispersion and absorption. Finally, note that both Y_r and Y_i are responsible for the resonant dielectric response (or the piezoelectric

behavior) of the sample. For small β, it follows from Eqs. (5), (9), and (10) that the resonance condition is met when the excitation frequency ω equals the frequency of the fundamental sound wave along the length of the sample. Furthermore, the larger β is, the broader the resonance width and the greater the shift of the resonance from the condition just mentioned. We may note from Eq. (5) that the viscosity η controls the value of β and, therefore, is an important parameter in the resonance phenomenon.

It is worth adding here a remark on the experimental conditions which has not been made in our earlier study[9] on KLT. Experimentally, one has the choice of measuring either the impedance (Z) or the admittance (Y) of sample. The capacitance and the dissipation factor are then derived from the measured Z or Y. In the present experiment, the capacitance and dissipation factor were measured in the series or impedance mode, while the above Eqs. (7) and (8) in the model correspond to the parallel or admittance mode. The real part of the permittivity ϵ'_{ser}, and dissipation D (or the loss tangent) for the series mode are related to ϵ' and ϵ'' for the parallel mode by

$$\epsilon'_{ser} = \frac{\epsilon'^2 + \epsilon''^2}{\epsilon'}, \tag{11}$$

$$D = \frac{\epsilon''}{|\epsilon'|}. \tag{12}$$

Far away from resonance, the measurements are insensitive to the chosen mode of operation. But, near the resonance, significantly different values can be obtained from the two distinct modes, particularly when the dissipation factor is large.

In the KLT paper mentioned previously,[9] Eqs. (7) and (8) for the permittivity and the dissipation factor were successfully used to fit the resonance data. From the fitting, an estimate of the electrostriction parameter M_{13} was obtained,[9] which was found comparable to the M_{13} value reported for PMN by Uchino *et al.*[14] In the next section, we present the experimental results for KTN and then use a similar fitting procedure to obtain estimates for the electrostriction parameter M_{13} and the relaxation time τ.

III. EXPERIMENTAL RESULTS

Measurements were made on KTN slab samples with 30% and 50% nominal Nb concentrations. The main surfaces were (100) surfaces, fully coated with aluminum electrodes and the measurements were made upon cooling . The largest dc bias field applied was approximately 400 V/cm and the small measuring field did not exceed 250 mV rms.

In Fig. 1 we show the dielectric constant (ϵ'/ϵ_0) for both samples as a function of temperature for 10 kHz and 1MHz. The three peaks correspond to the three transitions of the crystal structure to lower symmetries. KTN 30% [Fig. 1(a)] above 225 K and KTN 50% [Fig. 1(b)] above 255 K are paraelectric and hence macroscopically cubic. All the electrostriction measurements reported below were made in the

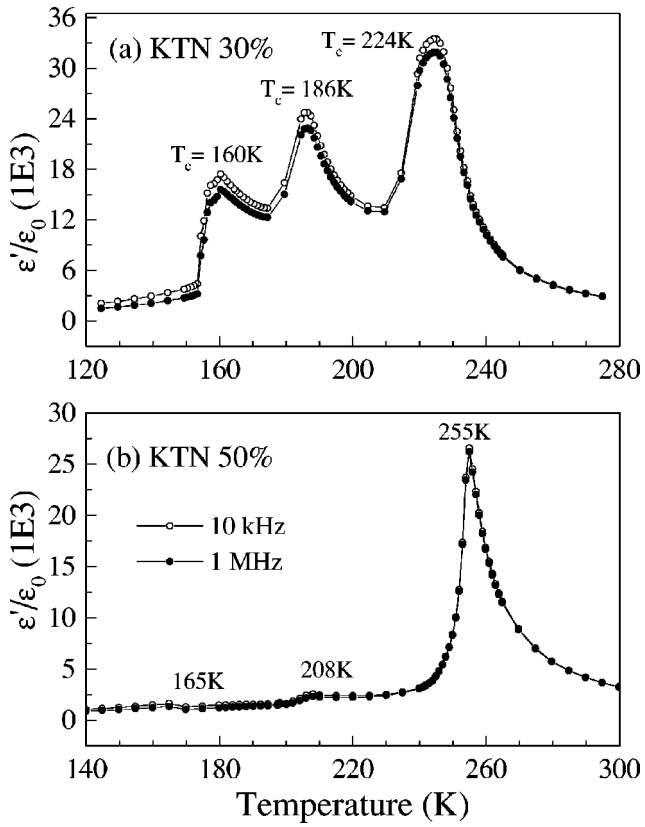

FIG. 1. The dielectric constant at 10 kHz and 1 MHz as a function of temperature: (a) KTN 30% and (b) KTN 50%. The peaks at 224 K in (a) and 255 K in (b), mark the cubic to tetragonal transition. Note that dispersive effects are only visible close to the transition.

paraelectric phase. In Fig. 1, it is important to note that, for both concentrations, the frequency dispersion is negligible until close to the transition temperature, indicating that the Nb reorientation takes place at a much higher frequency than the resonance, which occurs between 500 kHz and 1 MHz.

In Figs. 2(a) and 2(b) we show the dielectric resonance (in units of ϵ_0) measured on the 30% sample at 260 K and 240 K, respectively. We note that the absorption is slightly asymmetric at both temperatures and that its width decreases with temperature. More significantly, the strength of the absorption is seen to increase approximately six times more rapidly than the decrease of its width. By contrast, the dielectric constant does not increase in the same proportion. Figures 2(c) and 2(d) show that the 50% sample exhibits similar trends. We have calculated ϵ' and ϵ'' (in the units of ϵ_0) using Eqs. (11) and (12) to fit the experimental data at all temperatures. The solid lines in Figs. 2(a) and 2(d) are the calculated values and they agree reasonably well with the data. The fitting parameters have been provided in Table I and are discussed in the next section. It is important, however, to mention that, as τ was decreased, the fits got progressively better but also progressively less sensitive to the particular value of the relaxation time. Consequently, we can only quote an upper limit of 10^{-9} s for the Nb relaxation time, which is consistent with the very fast relaxation expected and mentioned earlier. The absorption peak for both

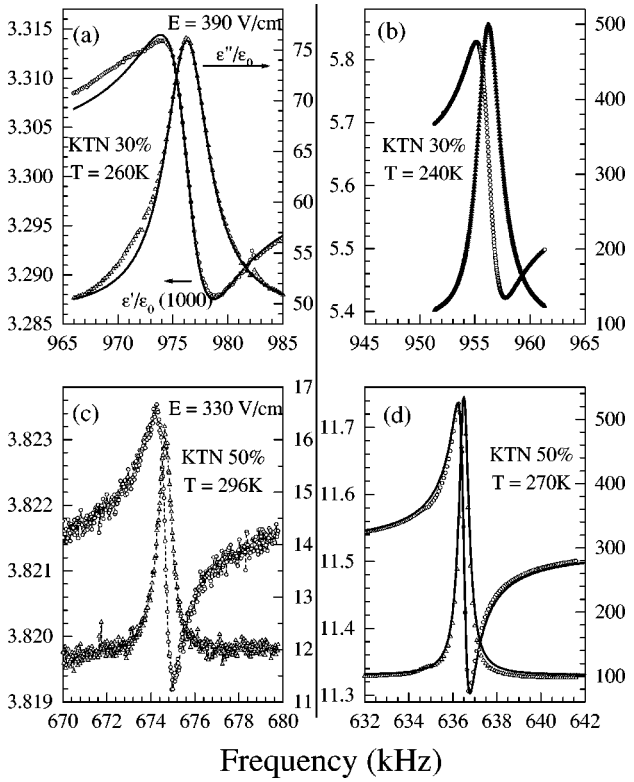

FIG. 2. Real (left axis and open circles) and imaginary (right axis and open triangles) parts of the dielectric response as a function of frequency: (a) KTN 30% at 260 K and (b) at 240 K; (c) KTN 50% at 296 K and (d) at 270 K. Note the increase of the absorption in both samples and also the shift of the absorption peak (in the units of ϵ_0) to lower frequency as the temperature is decreased. Solid line in (a) and (d) is the fit of Eqs. (11) and (12) to the data.

samples is also seen to shift to lower frequencies with decreasing temperature, as shown explicitly in Fig. 3. A similar decrease is observed for both concentrations, which is consistent with the reported softening of the elastic stiffness constant in KTN upon approaching the transition.[8]

From Eqs. (7) and (8), we note that both ϵ' and ϵ'' increase as the square of the external bias field, typical of electrostriction. In order to verify this dependence, measurements were conducted on both samples at a fixed temperature for different bias fields up to 400 V/cm. The result of a typical measurement are shown in Fig. 4(a) for the 30%

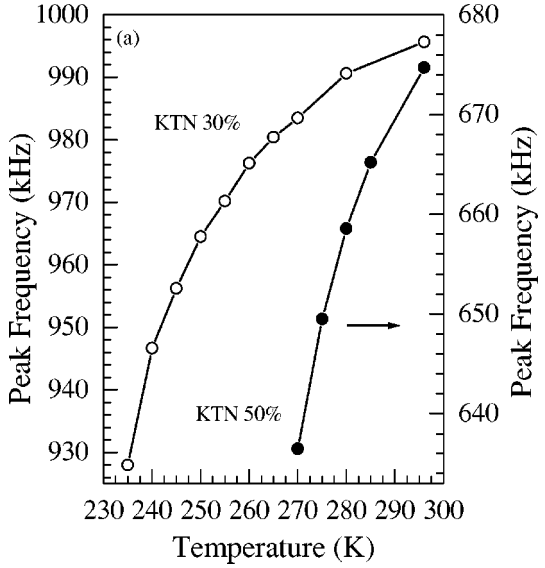

FIG. 3. Shift of the absorption peak to lower frequencies with decrease of temperature. Downward shift is consistent with the reported [8] softening of the elastic constant in KTN near transition.

sample, and Fig. 4(b) explicitly confirms that the absorption does increase as the square of the dc field. The solid line is a linear fit to the data and the fitting parameters are given in the plot. Similarly, ϵ' was also experimentally found to increase as the square of the dc field. On the other hand, the resonance frequency and the width of the resonance peak (Q factor) did not show any dependence on the applied dc field.

The most remarkable observation of the present study was made upon approaching the transition, when repetitively sweeping the frequency of the ac field through the resonance. In the experiment, the time elapsed between sweeps was approximately 30 s. The result of a measurement made on KTN 30% at 230 K (T_c+6 K) and with a dc bias field of 360 V/cm is shown in Fig. 5. Figures 5(a) and 5(b) show the time evolution of the series dielectric constant and dissipation, respectively. Unlike what happens at higher temperatures or for lower dc fields, where the trace of the resonance simply repeats itself upon repetitive sweeps (except for minor fluctuations), here its magnitude increases steadily with each sweep. Moreover, after a certain number of sweeps, the resonance suddenly splits into two extremely sharp spikes. In the intermediate frequency range between these spikes, the series capacitance assumes negative values [Fig. 5(a)]. Moreover,

TABLE I. Calculated parameters [Eqs. (9) and (10)] at different temperatures for the electrostrictive coefficient, static, and high-frequency dielectric constants, the viscosity parameter.

Sample	Temperature (K)	τ (s)	M_{13} (m^2/V^2)	ϵ_s	η (Poise)
KTN 50%	296	0.16×10^{-9}	4.97×10^{-18}	3821	76
KTN 50%	270	0.16×10^{-9}	4.1×10^{-17}	11520	62.5
KTN 30%	260	0.16×10^{-9}	2.75×10^{-17}	3301	255
KTN 30%	235	0.16×10^{-9}	7.33×10^{-17}	9700	148

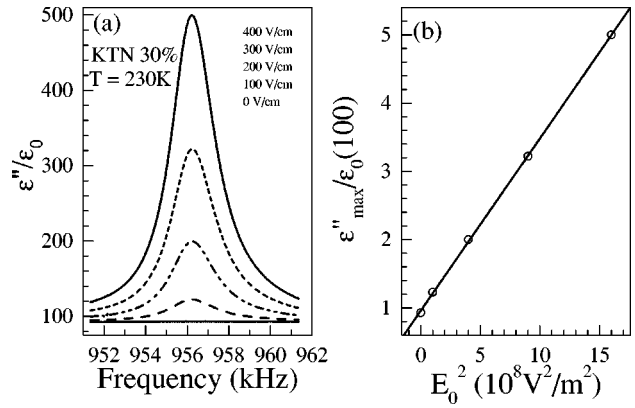

FIG. 4. (a) dc bias field strength dependence of the absorption peak. (b) Dependence of the peak absorption on the square of the bias field (solid circle). The solid line is the linear fit, expected from Eqs. (7) and (8).

with continued sweeping, the two sharp features move apart from each other, i.e., the frequency separation between them increases, eventually reaching a steady state value. For conventional piezoelectric crystals, such as quartz, these two singular responses are identified as a resonance and its antiresonance and they are separated by a fixed frequency difference. The original aspect of this phenomenon in KTN is its time evolution: starting from a single and broad resonance and evolving into a pair of very sharp resonance and antiresonance. Experimentally, we have also observed that the number of successive sweeps, required to provoke the splitting, decreases with increasing strength of the dc bias field and with decreasing temperature. A set of measurements on the 50% is also shown in Figs. 5(c) and 5(d) at 260 K (T_c $+5$ K) with a bias field of 230 V/cm. Here the field applied was smaller and, accordingly, more sweeps or a longer time was required to reach the splitting.

In order to understand the remarkable phenomenon just

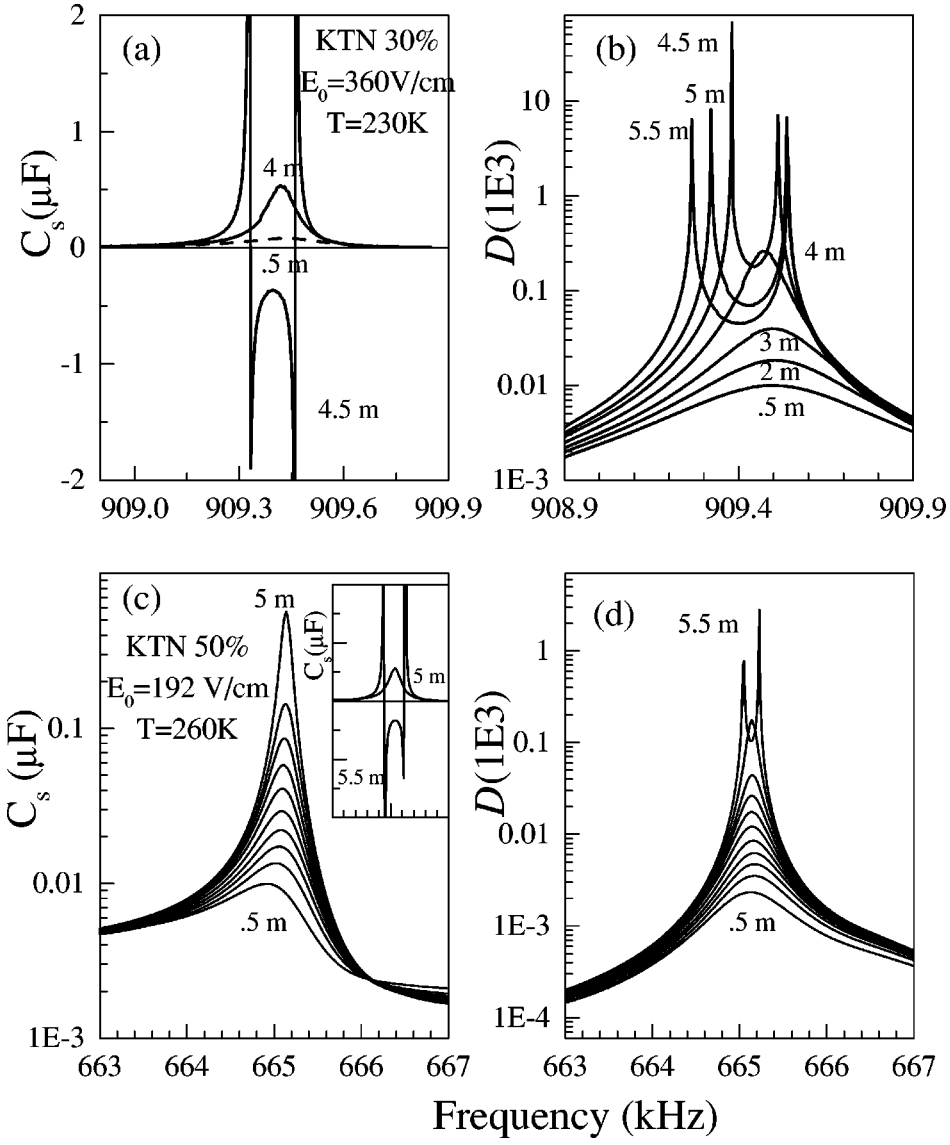

FIG. 5. Repetitive frequency traces of KTN 30% for (a) the series capacitance C_s and (b) the dissipation factor at 230 K with a bias field of 360 V/cm. Note that from the start to 4 min, both C_s and D increase steadily. In the next trace approximately half a minute later, both split and peak at enormously large values, indicating a singular behavior. (c) and (d) are similar traces for the KTN 50% but with a smaller dc bias field, showing the growth in more detail.

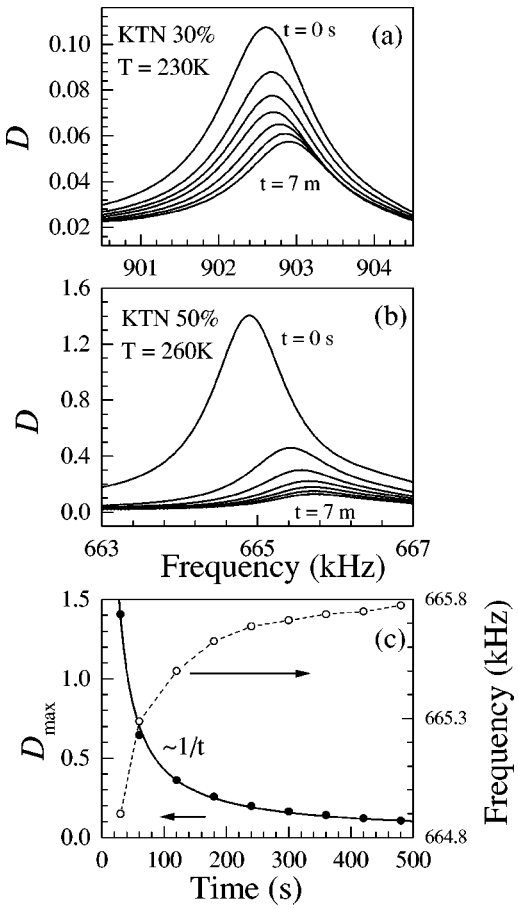

FIG. 6. Metastable piezoelectric behavior about 5 K above T_c for (a) KTN 30% and (b) KTN 50%. The traces are taken approximately 1 min apart. In both cases the dissipation decreases with time and the peak shifts to higher frequency. (c) Peak dissipation (solid circles) and the corresponding frequency as a function of time from (b) for the KTN 50% sample. The sold line is the hyperbolic fit to the dissipation ($D_{\max} \sim 1/t$).

described, it is useful to report another set of results relative to the time evolution or metastability of the resonance upon removal of the dc bias field but continued repetitive frequency sweeps of the small ac measuring field. The dissipation factor at successively later times, close to but above T_c is shown in Figs. 6(a) and 6(b) for both concentrations. Several significant points can be noted in these figures. First, after removal of the dc bias field, the magnitude of the resonance is smaller and its width larger. Second, the resonance starts approximately ten times stronger but decays faster in the 50% sample than in the 30% sample. In addition to a reduction in strength, the dissipation peak also shifts to higher frequency, and more so for the 50% sample. In Fig. 6(c) we present the time evolution of the dissipation maximum and that of the resonance frequency for the results in Fig. 6(b). As shown by the fit (solid line) to the data, the dissipation maximum closely follows a $1/t$ time dependence. The slow decay of the resonance upon removal of the dc bias field clearly reflects a certain degree of metastability of the macroscopic polarization.

IV. DISCUSSION

We first provide a qualitative explanation of the results, then use the model described earlier to illustrate our explanation and, finally, extract quantitative information. As in KLT, the observation of a dielectric resonance in KTN is linked to the presence of polar nanoregions. In fact, for all concentrations, the resonance appears 20–30 K above the transition, i.e., at a temperature where polar nanoregions have been shown to form.[7] As was discussed in two previous papers,[8,7] these polar nanoregions and their associated local strain fields mediate the coupling between macroscopic polarization and macroscopic strain, giving rise to the dielectric or electrostrictive resonance. The dielectric resonance results presented above also reveal the very dynamic character of the polar nanoregions in KTN. When turning on a dc bias field and repetitively sweeping the frequency of the small measuring ac field through the resonance, the induced polarization slowly builds up, increasing the strength and the Q factor of the resonance. When turning off the dc field, the induced polarization and the resonance slowly decay; the closer to T_c the faster the growth or the slower the decay.

Because of the very nature of the resonance, it is obvious that strain plays an essential role in both the growth and the decay of the polarization. The large width or low Q factor of the resonance for small dc fields suggests that competing local strain fields initially dampen or clamp the resonance. Sufficiently close to T_c, and upon repetitive frequency sweeps, the macroscopic strain from the electrostrictively driven vibration of the sample acts to further align the local strain fields. The metastability of this alignment allows for a cumulative buildup of the macroscopic polarization, itself leading to an even greater electrostrictive macroscopic strain, further stabilization of the macroscopic polarization. Provided the metastability time of the macroscopic polarization is longer than the sweep time, the resonance will increase in magnitude and in Q with each successive sweep. After a certain number of sweeps or, equivalently, once the strain-induced polarization exceeds a certain level, the resonance splits in two spikes, a resonance and an antiresonance. As will be shown below, in the intermediate frequency range between them, the electrostrictive or strain-induced contribution to the dielectric constant is greater than the dipolar contribution. Because the two contributions are out of phase, they have opposite sign and the net dielectric constant in that range is, therefore, negative.

In order to verify the validity of the previous qualitative explanation, we have carried out test calculations and then fitted the formulas given in the theory section to the experimental resonance curves.

A Possible Explanation for the Singular Response

From Eq. (7), we note that the total permittivity ϵ' can be written as the sum of a dipolar contribution ϵ_D, and an electrostrictive or strain-induced contribution ϵ_S,

$$\epsilon'(\omega) = \epsilon'_D(\omega) - \epsilon'_S(\omega), \tag{13}$$

where

$$\epsilon_D' = \frac{\epsilon_s + \epsilon_\infty \omega^2 \tau^2}{\omega^2 \tau^2 + 1}, \tag{14}$$

$$\epsilon_S' = f \frac{1 - Y_r(\omega) - \omega \tau Y_i(\omega)}{\omega^2 \tau^2 + 1}; \quad f = \frac{4E_0^2 M_{13}^2}{s_{11}^E}. \tag{15}$$

Because, in the KTN case, the relaxation time of Nb is very short, $\omega\tau \approx 0$ and ϵ_D' can be approximated by its static value, ϵ_s. In contrast, because Y_r given in Eq. (9) strongly depends on frequency, the strain-induced or electrostrictive contribution, ϵ_S', exhibits a large dispersion near the resonance frequency. The singular condition $\epsilon_S' = \epsilon_D'$, then becomes possible, for which both the series dielectric constant and the dissipation factor diverge [Eqs. (11) and (12)]. In KLT, $\epsilon_S' < \epsilon_D'$ over the whole frequency range of the resonance at all temperatures. In that case, the net dielectric constant remains positive throughout and the dielectric resonance does not exhibit any singular behavior. However, in KTN, the singular condition becomes fulfilled when the resonance is swept through repeatedly. We note from Eq. (15) that the only parameter that can undergo a progressive increase in the process is *f*, or more precisely M_{13}, since $1/s_{11}^E = \rho V^2$ is directly related to the resonance frequency that is not observed to change. Physically, what seems most plausible is that, repetitively sweeping through the resonance (where the vibration amplitude is maximum) overcomes more and more of the mutually competing internal strain fields and aligns a greater and greater number of the polar nanoregions. In the present formalism, this appears as an increase in the electrostriction coefficient. More accurately, the electrostriction coefficient can be said to depend on strain and the effect observed, described as a nonlinear electrostriction. The increase in *f* can then be accounted for by introducing a second-order electrostriction coefficient[12] in Eq. (1),

$$M_{13} \rightarrow M_{13}^0 + \gamma \Delta T_m(t), \tag{16}$$

where γ is a second-order coupling term and $\Delta T_m(t)$ is the additional stress that results from modulating the increasing strain-induced polarization. In a repetitive sweep, the strain-induced polarization increases, which, when modulated by the ac field, leads to an increase in the electrostrictive stress, $\Delta T_m(t)$, and a further increase in the vibrational amplitude or macroscopic strain.

In what follows, we have used Eqs. (11) and (12) along with Eq. (9), to carry out test calculations (in units of ϵ_0) illustrating the evolution of the dielectric constant and dissipation factor with time or, equivalently, increasing number of frequency sweeps through the resonance. Because repetitively sweeping through the resonance has the effect of building up the macroscopic polarization, different times in the calculation are equivalent to incrementing the value of *f* in Eq. (15). In Fig. 7(a), where $\epsilon_S' < \epsilon_D'$, the dissipation factor is small and does not exhibit a singular behavior. In Fig. 7(b), *f* has been increased so that the condition $\epsilon_S' = \epsilon_D'$ is now satisfied at two closely spaced frequencies and, accordingly, the dissipation factor splits into two spikes, with maximum values increased by more than three orders of magnitude. In Fig. 7(c), *f* has been increased further, so that ϵ_S' max is also greater and the ϵ_S' curve now intersects the ϵ_D' curve at two more widely separated frequencies.

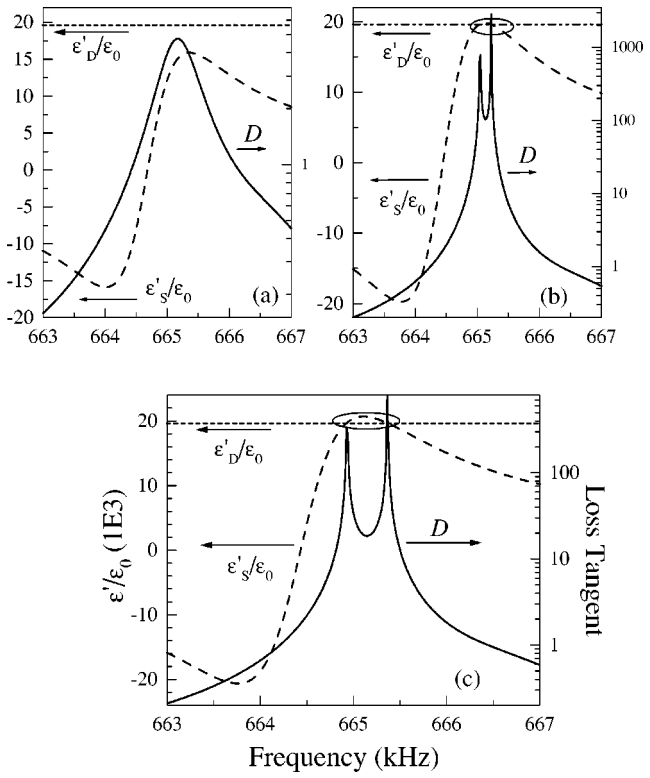

FIG. 7. The condition for singular response is met [see Eq. (13)] when ϵ_S' intercepts ϵ_D': (a) $\epsilon_S' < \epsilon_D'$ and correspondingly the loss tangent, *D*, does not exhibit any singular behavior. (b) ϵ_S' just intersects ϵ_D', leading to a closely spaced split in *D*. (c) approximately 2.5 min later, the intersecting points have moved apart, leading to a wider split.

We have used the above equations to fit the actual experimental data and to extract estimates for the electrostriction coefficient, M_{13}, and the relaxation time, τ. The results of the fits are shown in Figs. 8(a), 8(b), and 8(c) for KTN 50% at 260 K ($T_c + 5$ K) and for a dc bias field of 192 V/cm. The coupling parameter M_{13} increases progressively and is plotted in Fig. 8(d) as a function of time. It is seen to exhibit the following time dependence:

$$M_{13}(t) = a + b(1 - e^{-\frac{t}{\tau_m}}), \tag{17}$$

with $a = 9.95 \times 10^{-16}$ $\mathrm{m^2 V^{-2}}$, $b = 3.32 \times 10^{-16}$ $\mathrm{m^2 V^{-2}}$ and $\tau_m = 140$ s. Equation (17) is indeed of the form proposed earlier in Eq. (16). We may then associate *a* with the linear value, M_{13}^0, and the second term in Eq. (17) with the additional stress arising from the strain-induced polarization. In the experiment, M_{13} is found to saturate at a value that is about 33% higher than the initial value, M_{13}^0, i.e., $b/a \approx 0.33$. Further support for the above interpretation can be found in the result of a second measurement that was made at the same temperature but with a smaller bias field of 84

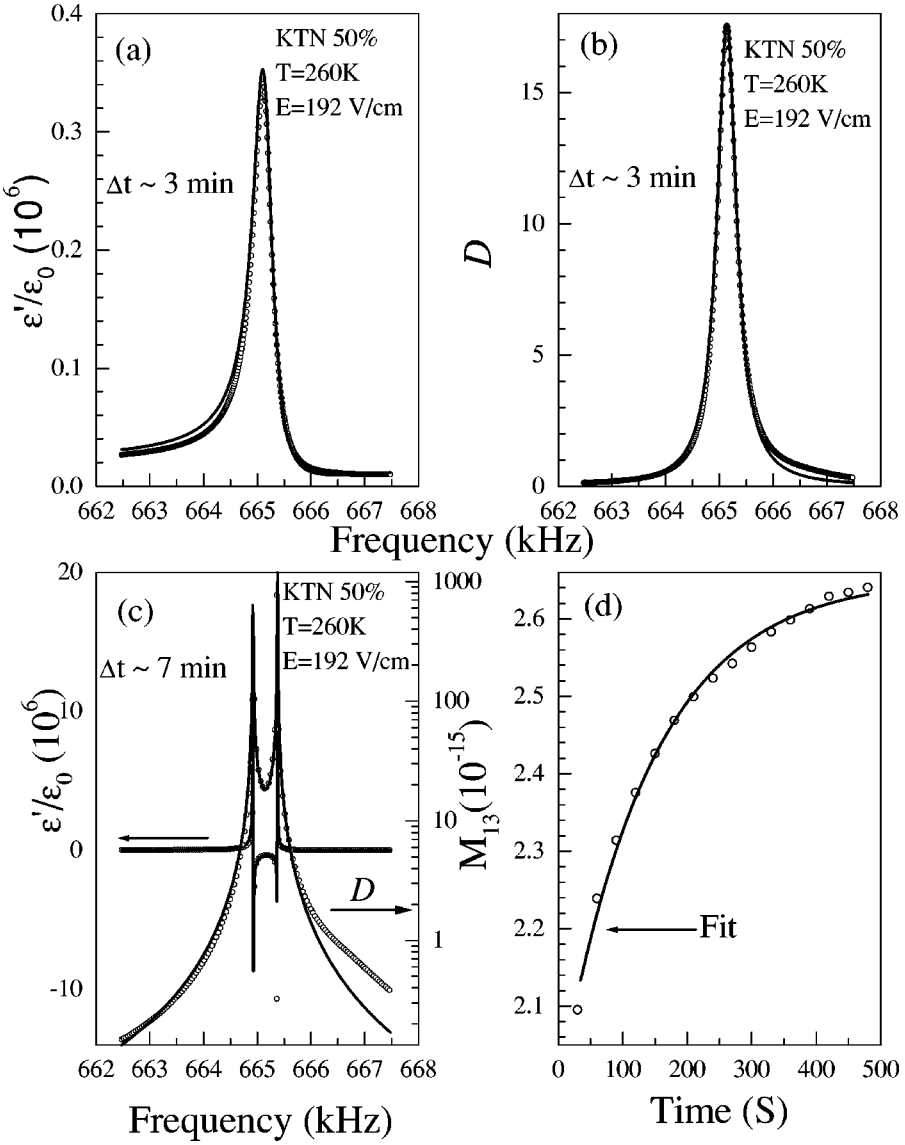

FIG. 8. Calculated (a) real dielectric constant and (b) loss tangent [from Eqs. (11) and (12)] compared with experimental results (open circles) for the KTN 50% crystal approximately 3 min after the first sweep. (c) A similar calculation compared with the experimental results after the split. This trace was then approximately 7 min after the first sweep. (d) The electrostrictive coupling parameter M_{13} used in the calculations (to obtain the best fit to the experimental results in the repetitive sweeps) is plotted against time (open circles). The solid line is the fit given by Eq. (17) in the text.

V/cm, for which the nonlinear contribution was expected to be much smaller and for which, indeed, no progressive growth of the resonance was observed. That second measurement yielded a value $M_{13}=1\times10^{-15}$, in good agreement with the value of a or M_{13}^0 obtained earlier.

The values obtained for the electrostriction coefficient, M_{13}, are given in Table I. They are found to be of the same order of magnitude as those in KLT but approximately 100 times larger than, e.g. those of $SrTiO_3$ and $BaTiO_3$. For $SrTiO_3$ at 243.3 K, M_{13} was reported by Rupprecht and Winter[15] to be $1.723\pm0.002\times10^{-19}$ m^2V^{-2} and for $BaTiO_3$ at room temperature, reported by Caspari and Merz[16] to be -3.33×10^{-19} m^2V^{-2}. The factor of 100 is consistent with the fact that, in their work, Caspari and Merz had to apply a bias field of 30 000 V/cm in contrast to 300 V/cm or less in our experiment on KTN. In Table I, M_{13} is also seen to increase with temperature but not to display any significant dependence on concentration.

We may also compare these values for the electrostriction coefficient of KTN with that of PMN. For ceramic PMN, Uchino *et al.*[14] reported a value of $M=1.92(\pm0.02)\times10^{-16}$ m^2V^{-2} (presumably at room temperature) measured with a driving voltage of 74.7 V_{rms} at 7 Hz corresponding to an rms driving electric field of about 200 V/cm since their sample was 3.68 mm thick. Comparatively, the value of M in KTN is about ten times smaller. However, KTN has the advantage that it can be operated at higher frequencies and with comparable or lower electric fields. Moreover, the Nb concentration can be adjusted, making KTN suitable for use as a transducer at lower temperatures.

Fitting Eqs. (11) and (12) to the data also provided, for both concentrations, an upper estimate of 10^{-9} s for the relaxation time τ of Nb in the polar nanoregions. In terms of a frequency, this is more than three orders of magnitude higher than the frequency at which the resonance occurs. As a consequence, Nb and the polar nanoregions can reorient almost instantaneously in response to the strain-induced order, and the Nb relaxation has little influence on the overall character of the resonance. This can be contrasted with KLT in which the Li polar nanoregions reorient at a much lower frequency.[9]

The other parameter that enters into the model is the phenomenological viscosity parameter, η in Eq. (2), which determines the width of the resonance. Consistent with the greater width of the resonance for KTN 30% (Fig. 2), η from the fit is found to be approximately three and half times greater for this concentration than for KTN 50%. In the same figure, the width of the resonance is also seen to decrease with temperature, and more so for KTN 30%. This suggests that the resistive or viscous drag force responsible for the absorption decreases with temperature. The smaller and more numerous polar regions, reorienting independently at higher temperature, provide a greater viscous drag force on one another, resulting in the broader width of the absorption. As the temperature decreases, the elastic constant also decreases, indicating a softening of the lattice. The polar regions increase in size and their mutual interactions grow stronger, weakening the viscous drag force and resulting in a narrower absorption. The narrower absorption width in the 50% sample is most likely due to the fact that, for higher concentrations, the polar regions are larger, behave more cooperatively and can, therefore, be more easily aligned. Because of a certain degree of metastability, the removal of the external dc bias field results in a slow decay of the macroscopic polarization and associated resonances, but not in a complete loss of alignment of the polar regions.

Finally, in Table I, the static dielectric constant is seen to increase with decreasing temperature, as expected.

V. CONCLUSIONS

In the present paper, we have reported experimental and theoretical results on the field-induced dielectric resonance in the mixed ferroelectric KTN. Such resonances are well known in conventional ferroelectric crystals such as $BaTiO_3$, in which the macroscopic polarization arises from the alignment of large domains in the ferroelectric phase and, therefore, requires large dc bias fields. However, in the case of KTN and KLT, the macroscopic polarization arises from the alignment of polar nanoregions that can be induced, in the paraelectric phase, by very modest bias fields ($\sim$100 smaller than in conventional ferroelectrics). Both qualitative and quantitative analyses of the resonance concur to show that, in KTN, this resonance is the manifestation of a strong electrostrictive coupling between macroscopic polarization and a macroscopic strain mediated by the polar nanoregions. A theoretical model has been developed and fitting to the experimental results has provided estimates for the essential parameters of the problem. For KTN, the electrostriction coefficient is found to be approximately 100 times larger than in conventional ferroelectrics and the relaxation time for reorientation of the off center Nb ions or of the polar nanoregions shorter than 10^{-9} s. Away from the transition, this resonance is broad or damped by competing local strain fields or internal friction between regions. When approaching the transition, and upon repetitive frequency sweeps, a remarkable growth in the magnitude and Q of the single resonance is observed, ending in an even more remarkable split into a resonance/antiresonance pair of extremely sharp spikes. This phenomenon is attributed to a feedback process between macroscopic polarization and macroscopic strain, helped by a certain degree of metastability of the polarization. It can be described as nonlinear electrostriction. Similar resonances have been observed in other relaxors and may exhibit a similar evolution when repetitively excited.

We gratefully acknowledge L. A. Boatner for providing the KLT and KTN single crystals. This work was partly supported by NSF Grant No. DMR. 9624436.

[1] U. T. Höchli, K. Knorr, and A. Loidl, Adv. Phys. **39**, 405 (1990).
[2] B. E. Vugmeister and M. D. Glinchuk, Rev. Mod. Phys. **62**, 938 (1990).
[3] O. Hanske-Petipierre and Y. Yacoby, Phys. Rev. B **44**, 6700 (1991).
[4] B. E. Vugmeister, P. DiAntonio, and J. Toulouse, Phys. Rev. Lett. **75**, 1646 (1995).
[5] P. DiAntonio, B. E. Vugmeister, J. Toulouse, and L. A. Boatner, Phys. Rev. B **47**, 5629 (1993).
[6] K. B. Lyons, P. A. Fleury, and D. Rytz, Phys. Rev. Lett. **57**, 2207 (1986).
[7] J. Toulouse and R. Pattnaik, J. Phys. Chem. Solids **57**, 1473 (1996).
[8] L. A. Knauss, R. Pattnaik, and J. Toulouse, Phys. Rev. B **55**, 3472 (1997).
[9] R. Pattnaik and J. Toulouse, Phys. Rev. B **60**, 7091 (1999).
[10] W. P. Mason in *Crystal Physics of Interaction Processes* (Academic Press, New York, 1966).
[11] Thrygve Meeker, in *Precision Frequency Control*, edited by Edward A. Gerber and Arthur Ballato (Academic Press, New York, 1985), Vol. 1.
[12] Takuro Ikeda, in *Fundamentals of Piezoelectricity* (Oxford University Press, London, 1990).
[13] H. F. Pollard, in *Sound Waves in Solids* (Pion, London, 1977).
[14] K. Uchino, S. Nomura, L. E. Cross, R. E. Newnham, and S. J. Jang, J. Mater. Sci. **16**, 569 (1981).
[15] G. Rupprecht and W. H. Winter, Phys. Rev. **155**, 1019 (1967).
[16] M. E. Caspari and W. J. Merz, Phys. Rev. **80**, 1082 (1950).